Total electron-impact ionization cross-sections of CF_x and NF_x (x=1-3)

Winifred M. Huo[a1], Vladimir Tarnovsky[b] and Kurt H. Becker[b]

[a] NASA Ames Research Center, Mail Stop T27B-1, Moffett Field, CA 94035-1000

[b] Department of Physics, Stevens Institute of Technology, Hoboken, NJ 07030

Abstract

The discrepancy between experimental and theoretical total electron-impact ionization cross-sections for a group of fluorides, CF_x and NF_x (x=1-3), is attributed to the inadequacies in previous theoretical models. Cross-sections calculated using a recently developed siBED model that takes into account the shielding of the long-range dipole potential between the scattering electron and target are in agreement with experiment. The present study also carefully re-analyzed the previously reported experimental data to account for the possibility of incomplete collection of fragment ions and the presence of ion-pair formation channels. For NF_3, our experimental and theoretical cross-sections compare well with the total ionization cross-sections recently reported by Haaland et al. in the region below dication formation.

[1] Corrresponding author. Fax: +1-650-604-0350; email: whuo@mail.arc.nasa.gov.

1. Introduction

Electron-impact ionization of atoms and molecules is a fundamental process in any plasma. Large experimental databases for electron-impact ionization cross-sections for a number of molecules are now available [1]. However, measurements of reactive species such as radicals are known to be difficult. Essentially all available measured ionization cross sections for free radicals were obtained by the fast-neutral-beam technique which was pioneered by Freund and co-workers [2] and subsequently used extensively by Becker and co-workers [3]. Theoretically, *ab initio* calculations present a challenging problem and currently are limited to atoms. For molecules, two physically based models, the binary-encounter Bethe (BEB) model of Kim and Rudd [4] and the semiclassical Deutsch-Märk model (DM model) [5] have provided efficient means for the determination of ionization cross-sections. The cross-sections determined using both models are in generally good agreement with experiment and with each other. However, for a group of fluorines, CF_x and NF_x (x=1-3), discrepancies between 50% to 100% are found when compared with the experimental data of Tarnovsky et al. [6-9]. This is a surprising result in view of the good agreement obtained for many molecules. Also, the ionization cross-sections of NF_3 from the recent measurement by Haaland et al. [10] using Fourier Transform Spectroscopy are in good agreement with the data of Tarnovsky et al. [8] except in the region of dication formation. This result lessens the probability that experimental problems are responsible for the observed discrepancy. Up to the now, no adequate explanation has been proposed for the difference between theory and experiment.

Both CF_x and NF_x are important gases in semiconductor processing. All three CF_x are very reactive. They and their ions are responsible for most gas phase and surface reactions in fluorocarbon plasmas. Nitrogen trifluoride is used both in plasma etching and in thermal cleansing of semiconductors and liquid crystal display panels. In view of the importance of these fluorides in industrial applications, we have carried out a combined theoretical and experimental study of the electron-impact ionization of these molecules. This study should also improve our fundamental understanding of electron-molecule collisions.

The group of molecules in this study shares two common features: they only have fluorine bonds and the non-fluorine atom has nonbonding valence electrons. While the charge distribution of a nonbonding electron usually centers near the atomic nucleus, in this case the strongly polar fluorine bond pulls the electron into the bonding region, resulting in a built-up of charge there. In

a theoretical model of electron collisions with this group of fluorides, the strong repulsive field in the bonding region must be taken into account in order to describe the collision process properly.

Recently one of us has developed an improved binary-encounter dipole (iBED) model [10] for electron-impact ionization of atoms and molecules. In this model, the long-range dipole interaction between the electron and target is represented by the dipole Born cross-section, instead of the dipole Bethe cross-section as in the BED model. Furthermore, the dipole potential is properly shielded as the electron approaches the bonding region. When the optical oscillator strength (OOS) for the dipole transition is not known, a simplifed version of the iBED model (siBED) is introduced that uses an approximate OOS based on the f-sum rule. If the inadequate description of the dipole interaction potential is indeed the source for the discrepancies between theory and experiment, then the iBED/siBED model should be capable of reconciling the difference.

A brief outline of the iBED/siBED model is presented in Sec. 2 together with the determination of the shielding and molecular parameters. The re-analysis of the experimental data is presented in Sec. 3. The experimental and theoretical cross-sections are compared in Sec. 4 and Sec. 5 concludes our results.

2. Theoretical treatment

Consider the spherical harmonics expansion of the Coulomb potential

$$\frac{1}{|r_o - r_i|} = \sum_{\lambda}\sum_{\mu} \frac{4\pi}{2\lambda+1} \frac{r_<^{\lambda}}{r_>^{\lambda+1}} Y^*_{\lambda\mu}(\Omega_o) Y_{\lambda\mu}(\Omega_i). \qquad (1)$$

The dipole term is given by

$$\sum_{\mu} \frac{4\pi}{3} \frac{r_<}{r_>^2} Y^*_{1\mu}(\Omega_o) Y_{1\mu}(\Omega_i), \qquad r_< = (r_o, r_i)_<, r_> = (r_o, r_i)_> \qquad (2)$$

When the scattering electron is outside the molecular charge cloud, the dipole potential is described by

$$\sum_{\mu} \frac{D_{\mu}}{r_o^2} Y_{1\mu}^*(\Omega_o), \tag{3}$$

with D_u one component of the transition dipole moment. When the scattering electron is inside the molecular charge cloud, the interaction potential changes to

$$\sum_{\mu} B_{\mu}(r_o) r_o Y_{1\mu}^*(\Omega_o), \tag{4}$$

where $B_{\mu}(r_o)$ is given by

$$B_{\mu}(r_o) = \frac{4\pi}{3} \int_{r_o}^{\infty} dr_i r_i^2 \int d\Omega_i \frac{Y_{1\mu}(\Omega_i)}{r_i^2} \rho_{po}(r_i \Omega_i). \tag{5}$$

Here $\rho_{po}(r_i\Omega_i)$ is the transition charge density of the target. Eqs. (3) and (4) show that the dipole potential changes character when the scattering electron penetrates inside the molecular charge cloud. The potential in Eq. (3) is the long-range dipole potential, and the short-range potential in Eq. (4) can be considered a shielding potential because it prevents the long-range potential in Eq. (3) from diverging at $r_o = 0$. Note that the dipole Bethe cross-section used in the BED model [3] to describe dipole interaction is a high-energy approximation. At the limit of very high energies, only glancing collisions are important. Thus the dipole Bethe cross-section only accounts for the long-range dipole interaction in Eq. (3), but not the short-range shielding of the dipole potential in Eq. (4).

For the ionization of an electron out of the orbital o in the target to the ion state p, the iBED cross-section is given by

$$\sigma_{po}^{iBED} = \sigma_{po}^{dB} + \sigma_{po}^{BE}. \tag{6}$$

Here σ_{po}^{dB} is the dipole Born cross-section and σ_{po}^{BE} is a modified Mott cross-section with the incident electron energy replaced by the average energy from the binary-encounter model. The Mott cross-section is a generalization of the Rutherford cross-section for Coulomb scattering by taking into account exchange. The direct term in the Mott cross-section is associated with the $\lambda=0$ term in Eq. (1). σ_{po}^{BE} is referred to as the binary-encounter cross-section by Kim and Rudd [4] but is different from the binary-encounter cross-section of Vriens [11]. It is given by

$$\sigma_{po}^{BE} = \frac{4\pi N_o}{k_o^2 + \kappa_o^2 + \alpha_o^2}\left[\frac{k_o^2 - \alpha_o^2}{k_o^2 \alpha_o^2} - \frac{1}{k_o^2 + \alpha_o^2}\ln\left(\frac{k_o^2}{\alpha_o^2}\right)\right]. \tag{7}$$

Here N_o is the occupation number of the orbital, α_o is twice the magnitude of its binding energy, κ_o^2 twice its kinetic energy, and k_o the momentum of the incoming electron.

The dipole Born cross-section is represented by a three-term polynomial derived from a series representation for the generalized oscillator strength (GOS) of electron impact ionization. The series representation for the GOS is the ionization analog of the Lassettre series for bound-bound transitions [12]. This representation not only describes the long-range dipole interaction of the electron and target, but also the shielding of the dipole field as the scattering electron comes inside the bonding region. The use of the dipole Born cross-section also removes the empirical energy-scaling factor in the BED model. The following expression for the dipole Born cross-section is used in the iBED model,

$$\sigma_{po}^{dB} = \int_0^{(k_o^2 - \alpha_o^2)/2} dE_p \frac{8\pi(k_p^2 + \alpha_o^2)^5}{k_o^2} \frac{df_{po}^{(o)}}{dE_p} \int_{K_{\min}}^{K_{\max}} dK \frac{(1 + d_1 t + d_2 t^2) dK}{K[(K + k_p)^2 + \alpha_o^2]^3[(K - k_p)^2 + \alpha_o^2]^3}. \tag{8}$$

Here E_p and k_p are the energy and momentum of the ejected electron, W_{po} the excitation energy, K the momentum transfer of the scattering electron, and $df_{po}^{(o)}(E_p)/dE_p$ the optical oscillator strength (OOS) for the corresponding photoionization process. The parameters d_1 and d_2 are related to the shielding of the dipole potential, and the variable t is given by

$$t = \frac{K^4}{[(K+k_p)^2+\alpha_o^2][(K-k_p)^2+\alpha_o^2]}. \tag{9}$$

The total single ionization cross-section of a molecule is given by

$$\sigma_{iBED} = \sum_o \sum_p \sigma_{po}^{iBED}. \tag{10}$$

The calculation of iBED cross-sections requires the OOS for the corresponding photoionization process, the binding energy and the kinetic energy of the electron being ejected, and the shielding parameters d_1 and d_2. In the case when the OOS is not available, an approximation expression has been proposed based on the *f*-sum rule [10].

$$\frac{df_{po}^{(o)}(E_p)}{dE_p} = \frac{8\alpha_o^2 N_o k_p}{\pi(k_p^2+\alpha_o^2)^6}. \tag{11}$$

In the simplified version of the iBED model (siBED), Eq. (11) is used to represent the OOS. The siBED model is used for all CF_x and NF_x calculations reported in this paper.

2.1 Choice of d_1 and d_2

In principle, d_1 and d_2 can be calculated using the interaction potential in Eq. (4), with $B_\mu(r_o)$ determined using Eq. (5) and the transition density ρ_{po} deduced from target wave functions. However, for molecular wave functions represented by a Gaussian basis set, the partial integral in Eq. (5) is not in closed form. In Ref. 9, a different approach is used to determine d_1 and d_2. For N_2 and CH_4, the two parameters were determined empirically based on the optimal representation of the experimental data of Straub et al. [13, 14] and Rapp and Englander-Golden [15] using the iBED model [10]. (Note that a recent recalibration of the apparatus by the Rice group results in data that differ slightly from those in the original publication [16]). For both N_2 [10] and CO [17], the optimal choice of the two parameters are $d_1 = -2.0$, $d_2 = 0.4$. The parameter d_1 is found to be important to in determining the shape and magnitude of the cross-

sections near the peak of the cross-section versus energy curve. The negative value denotes a repulsive correction to the purely attractive long-range dipole potential as the scattering electron enters the molecular charge cloud. The parameter d_2 does not play any significant role until the incident electron energy is above 100 eV. It provides a small attractive correction to d_1 as the scattering electron moves close to the nuclear centers.

In the present study, we determine d_1 and d_2 by comparing the molecular property f_e for CF and NF with CO. The property f_e is defined by

$$f_e = \int_0^\infty dr_i r_i^2 \int d\Omega_i \frac{\cos\theta_i}{r_i^2} \rho_{oo}(r_i\Omega_i). \qquad (12)$$

Note that the f_e closely resembles the expression $B_\mu(r_o)$ in Eq. (5) that determines the short-range shielding potential. While $B_\mu(r_o)$ uses the transition density ρ_{po} and the integration over r_i is over a limited range, f_e is defined by the density ρ_{oo} of the initial target state and the r_i integration covers the full space. How f_e changes from CO to the fluorides may serve as an indicator how $B_\mu(r_o)$, and consequently d_1, should be modified. Table I compares the values of f_e for the valence orbitals of CF and CO, and for NF and CO. The orbitals are determined using complete-active-space self-consistent-field (CASSCF) calculations. These calculations used the aug-cc-pVQZ basis of Gaussian functions [18]. The active space used in the CASSCF calculations is (6,3,3,0) for CF and NF and (6,2,2,0) for CO. To eliminate variations in f_e due to the difference in geometry, the experimental geometry of CF is used in the calculation for the CF/CO comparison and the NF/CO comparison uses the experimental geometry of NF. Table 1 shows that the orbital f_e's for CF and NF, with one exception, are close to a factor of 2 larger than the corresponding f_e's for CO. Based on this result, and similar results from the comparison of the orbital f_e's of CF_2 and NF_2 with CO_2, and CF_3 and NF_3 with BF_3, we determine that the increase shielding in this group of fluorides can be represented by scaling the d_1 parameter by a factor of 2.4. Thus $d_1 = -4.8$ is used in our fluoride calculations.

There is little guidance available in choosing the parameter d_2. However, the role of d_2 is insignificant until the incident electron energy is above 100 eV. We slightly modify the d_2 of CO to reflect the diminished attractive potential in the inner region of the fluorides and use $d_2 = 0.3$.

2.2 Calculation of molecular parameters

The binding energies and kinetic energies of the target electrons have been determined using quantum chemistry calculations. All calculations use the experimental geometry of the neutral molecules. The calculations for CF, CF_2, NF, and NF_2, employ the aug-cc-pVQZ basis of Gaussian functions and the aug-cc-pVTZ basis for CF_3 and NF_3. The kinetic energies of the target electrons, $\kappa_o^2/2$, are directly calculated using Hartree-Fock functions. On the other hand, the binding energies $-\alpha_o^2/2$ are sensitive to correlation effects. For valence electrons, they are determined by taking the energy difference between the neutral target state and the ion. Since the calculations are done at the equilibrium geometry of the target, they are just the vertical ionization potential (VIP) associated with the ion states. The RCCSD(T) method (symmetry restricted couple-cluster singles and doubles with perturbation treatment of triples) [19,20] is used in the calculation of the lowest ion state of each symmetry. The RCCSD(T) method is size consistent and thus suited for the calculation of energy difference between systems with different number of electrons. However, RCCSD(T) can only be used to determine the lowest ion state of each symmetry. The energies of the second and higher ion states of a symmetry are determined using CASSCF calculations and the result is scaled by the difference between the CASSCF and RCCSD(T) result for the lowest state. The binding energies of the inner orbitals are determined from Hartree-Fock functions using Koopmans theorem. All quantum chemistry calculations have carried out using MOLPRO [21]. Table 2 presents the binding energies and kinetic energies for the fluorides. The data for the core orbitals are not listed because their contributions to the ionization cross-section are negligible in the energy range considered in this study. For CF_2, the binding energies of the $4a_1$, $5a_1$, and $3b_2$ electrons are taken from the compiled ionization potential data of Levin and Lias [22].

3. Analysis of experimental data

We carefully re-analyzed the originally reported experimental cross section data for all six free radicals in an effort to ensure that systematic effects that may influence the proper determination of the total single ionization cross sections are fully accounted for to the maximum extent possible. The total single ionization cross section for each free radical is obtained as the sum of all measured partial ionization cross sections. The sum of all partial ionization cross

sections for a given target will only yield the "correct" total single ionization cross section, if all channels leading to the formation of one singly charged positive ion are properly taken into account. This requires estimates for contributions to the total single ionization cross section from partial ionization channels whose cross sections were not or not accurately measured because of weak signals and/or significant excess kinetic energy that precludes a 100% collection of a specific fragment ion. Another issue is the presence of (positive) ion – (positive) ion pair formation processes whose contributions to the total single ionization cross section have to be discounted which requires that their respective absolute cross sections and energy dependences have to be determined or estimated. In the course of the present work we re-analyzed all original data files relating to the measurements of the CF_x and NF_x partial ionization cross sections in an effort to obtain the most reliable experimental total single electron impact ionization cross sections for these six free radicals.

4. Results

Figure 1 presents the total single ionization cross-sections calculated using the siBED model and the revised experimental values for CF, CF_2, and CF_3. Also presented are the theoretical cross-sections using the BEB model and the DM model. The corresponding data for NF, NF_2, and NF_3 are presented in Fig. 2. For NF_3 the data from the recent experiment of Haaland et al. [23] are also presented. Note that all BEB cross-sections have been calculated using the molecular parameters determined in this study. The cross sections therefore differ slightly from the BEB calculations reported by Kim and Irikura [24]. For all six molecules, the siBED cross-sections and the revised experimental cross-sections agree to within experimental error. For CF_2, CF_3, NF_2 and NF_3, the agreement is very good and the two sets of cross-section curves almost lie on top of each other. The agreement is less satisfactory for CF and NF where the siBED cross-sections are consistently larger than the experimental values. However, as pointed out in the original papers by Tarnovsky et al. [7,9], the atomic fragment ions resulting from the dissociative ionization of these two diatomic radicals are formed with significant excess kinetic energy. It is, therefore, difficult to quantify the collection efficiency of the fragment ions in these cases and the reported experimental ionization cross sections for NF and CF should be considered a lower limit [7,9]. Our cross-sections for NF_3 also agree well with the data of Haaland et al. [23] at 100 eV and below. It should be noted that the measurements of Haaland et al. includes the contributions from

all ionization processes, among them dication formation. For electron energies above the threshold of dication formation, the cross-section data of Haaland et al. should be larger than the corresponding total single ionization cross-sections. Thus their cross-sections and the cross-sections presented in this paper are no longer directly comparable at those energies. Also, as seen in Figs. 1 and 2, calculations using the BEB and DM models consistently overestimate the cross-sections for this group of fluorides.

5. Conclusions

The agreement between experiment and the siBED model suggests that the long-standing discrepancies between theory and experiment in the total single ionization cross-sections for CF_x and NF_x (x=1-3) are due to an inadequate description of the electron interaction potential in previous theoretical models.

Acknowledgements

W.M.H. acknowledges support from NASA program code 704-40-42. Two of us (V.T. and K.B.) acknowledge financial support from the Division of Chemical Sciences, Office of Basic Energy Sciences, Office of Science, U.S. Department of Energy. We are grateful to Prof. Hans Deutsch for providing us with tabulated values of the calculated DM ionization cross sections for the six free radicals studied in this paper.

References

[1] (a) L.G. Christophorou, J.K. Olthoff, M.V.V.S. Rao, J. Phys. Chem Ref. Data, 25 (1996) 1341. (b) *ibid*, 26 (1997) 1. (c) L.G. Christophorou, J.K. Olthoff, Yichang Wang,, , *ibid*, 26 (1997) 1205. (d) L.G. Christophorou, J.K. Olthoff, *ibid*, 27 (1998) 1. (e) *ibid*, 27 (1998) 889. (f) *ibid*, 28 (1999) 131. (g) *ibid*, 29 (2000) 553. (h) *ibid*, 29 (2000) 267. (I) *ibid*, 30 (2001) 449.

[2] F.A. Biaocchi , R.C. Wetzel, and R.S. Freund, Phys. Rev. Lett. 53 (1984) 771

[3] V. Tarnovsky, H. Deutsch, K.E.Martus, and K. Becker, J. Chem. Phys. 109 (1998) 6596 and references therein to earlier work

[4] Y.-K. Kim, M.E. Rudd, Phys. Rev. A 50 (1994) 3954.

[5] H. Deutsch, K. Becker, S. Matt, T.D. Märk, Int. J. Mass Spectrom. 197 (2000) 37.

[6] V. Tarnovsky, K. Becker, J. Chem. Phys. 98 (1993) 7686.

[7] V. Tarnovsky, P. Kurunczi, D. Rogozhnikov, K. Becker, Int. J. Mass Spectrom. Ion Processes 128 (1993) 181.
[8] V. Tarnovsky, A. Levin, K. Becker, R. Basner, M. Schmidt, Int. J. Mass Spectrom. Ion Processes 133 (1994) 175.
[9] V. Tarnovsky, A. Levin, K. Becker, J. Chem. Phys. 100 (1994) 5626.
[10] W.M. Huo, Phys. Rev. A (accepted for publication).
[11] L. Vriens, in *Case Studies in Atomic Physics*, edited by E.W. McDaniel and M.R.C. McDowell (North-Holland, Amersterdam, 1969). Vol. 1, 0.335.
[12] E.N. Lassettre, J. Chem. Phys. 43 (1965) 4479.
[13] H.C. Straub, P. Renault, B.G. Lindsay, K.A. Smith, and R.F. Stebbings, Phys. Rev. A 54 (1996) 2146.
[14] H.C. Straub, D. Lin, B.G. Lindsay, K.A. Smith, and R.F. Stebbings, J. Chem. Phys. 106 (1997) 4430.
[15] D. Rapp and P. Englander-Golden, J. Chem. Phys. 43 (1965) 1464.
[16] B.G. Lindsay and M.A. Mangan, in *Photon- and electron-interactions with molecules: Ionization and dissociation*, edited by Y. Itikawa Landolt-Börnstein, New Series, Group 1, Vol. 17, Pt C (Springer-Verlag, Berlin, in press).
[17] W.M. Huo, unpublished result.
[18] T.H. Dunning, J. Chem. Phys. 90 (1989) 1007; R.A.~Kendall, T.H. Dunning, and R.J. Harrison, *ibid* 96 (1992) 6796.
[19] P.J. Knowles, C. Hampel, and H.-J. Werner, J. Chem. Phys. 99 (1993) 5219.
[20] J.D. Watts, J. Gauss, and R.J. Bartlett, J. Chem. Phys. 98 (1993) 8718.
[21] MOLPRO is a package of *ab initio* program written by H.-J. Werner and P.J. Knowles with contributions from J. Almlöf et al.
[22] R.D. Levin and S.G. Lias, NBS Report No. NSRDS-NBS 71, (1982).
[23] P.D. Haaland, C.Q. Jiao, and A. Garscadden, 340 (2001) 479.
[24] Y.-K. Kim and K.K. Irikura, Proceedings of the Database Workshop.

Table 1. Comparison of the property f_e (au) for the valence orbitals of the CF/CO and for NF/CO pairs. Calculations are carried out at the experimental geometry of CF and NF, respectively.

Orbital	f_e			
	CF	CO	NF	CO
3σ	0.9665	0.4738	0.7230	0.4947
4σ	0.5595	-0.0974	-0.3091	-0.1285
5σ	-0.0577	0.4364	0.6524	0.4383
1π	0.8296	0.4152	0.7372	0.4070

Table 2. Binding energies ($-\alpha_o^2/2$) and kinetic energies ($\kappa_o^2/2$) used in the siBED calculations. Both quantities are in eV.

Orbital	CF ($X^2\Pi$)		NF ($X^3\Delta$)	
	$-\alpha_o^2/2$	$\kappa_o^2/2$	$-\alpha_o^2/2$	$\kappa_o^2/2$
3σ	46.804[a]	101.378	46.112[a]	98.804
4σ	23.304[b]	80.062	24.418[b]	78.282
5σ	13,985[c]	48.144	16.624[c]	70.199
1π	18.411[c]	81.922	17.913[c]	84.018
2π	9.475[c]	45.231	12.651[c]	60.703

Orbital	CF_2 (X^1A_1)		NF_2 (X^2B_1)	
	$-\alpha_o^2/2$	$\kappa_o^2/2$	$-\alpha_o^2/2$	$\kappa_o^2/2$
$3a_1$	47.674[a]	95.446	47.073[a]	92.903
$4a_1$	24.000[d]	82.088	29.489[a]	83.938
$5a_1$	19.200[d]	75.808	18.749[b]	74.653
$6a_1$	12.244[c]	55.719	14.716[c]	77.847
$1b_1$	19.241[c]	74.534	18.380[c]	79.830
$2b_1$			12.195[c]	68.900
$2b_2$	45.446[a]	106.832	44.668[a]	106.706
$3b_2$	22.200[d]	81.676	20.906[b]	78.274
$4b_2$	16.665[c]	95.114	16.273[c]	93.850
$1a_2$	17.298[c]	88.008	16.508[c]	89.544

Orbital	CF_3 (X^2A_1)	NF_3 (X^1A_1)

	$-\alpha_o^2/2$	$\kappa_o^2/2$	$-\alpha_o^2/2$	$\kappa_o^2/2$
$3a_1$	47.552[a]	93.051	48.828[a]	87.299
$4a_1$	26.400[a]	82.590	30.523[a]	89.586
$5a_1$	21.723[a]	75.316	23.018[a]	69.615
$6a_1$	11.056[c]	59.408	13.731[c]	81.082
$1a_1$	16.363[c]	94.458	16.180[c]	96.263
2e	45.250[a]	105.136	45.127[a]	106.502
3e	22.983[a]	76.776	23.190[a]	75.853
4e	18.224[b]	85.933	18375[b]	86.623
5e	17.590[c]	90.592	16.443[b]	93.111

[a]Hartree-Fock calculation based on Koopman's theorem.

[b]CASSCF calculation corrected by RCCSD(T) results.

[c]RCCSD(T) calculation.

[d]Compilation of Levin and Lias [22].

Figure captions

Figure 1. (a) Total single ionization cross-section of (a) CF, (b) CF_2 and (c) CF_3 calculated using the siBED model and the revised experimental data. Also presented are theoretical cross sections calculated using the BEB model of Kim and Rudd [4] and the DM model [5].

Figure 2. (a) Total single ionization cross-section of (a) NF, (b) NF_2 and (c) NF_3 calculated using the siBED model and the revised experimental data. Also presented are theoretical cross sections calculated using the BEB model of Kim and Rudd [4] and the DM model [5]. For NF_3 the cross-section data form the measurements of Haaland et al. [23] also are presented

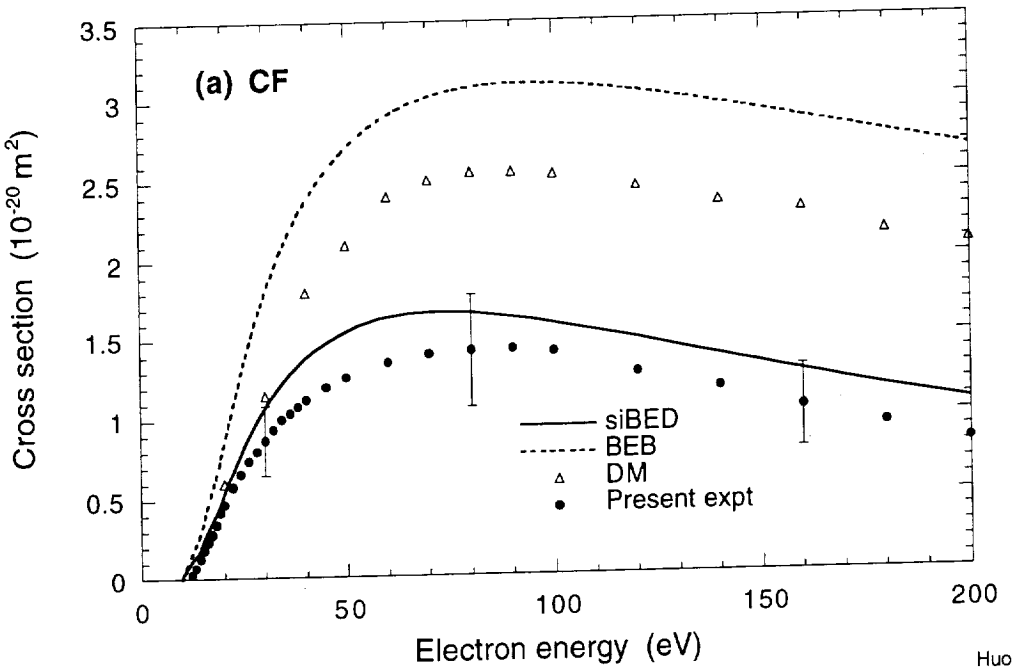

Huo et al. Fig. 1a

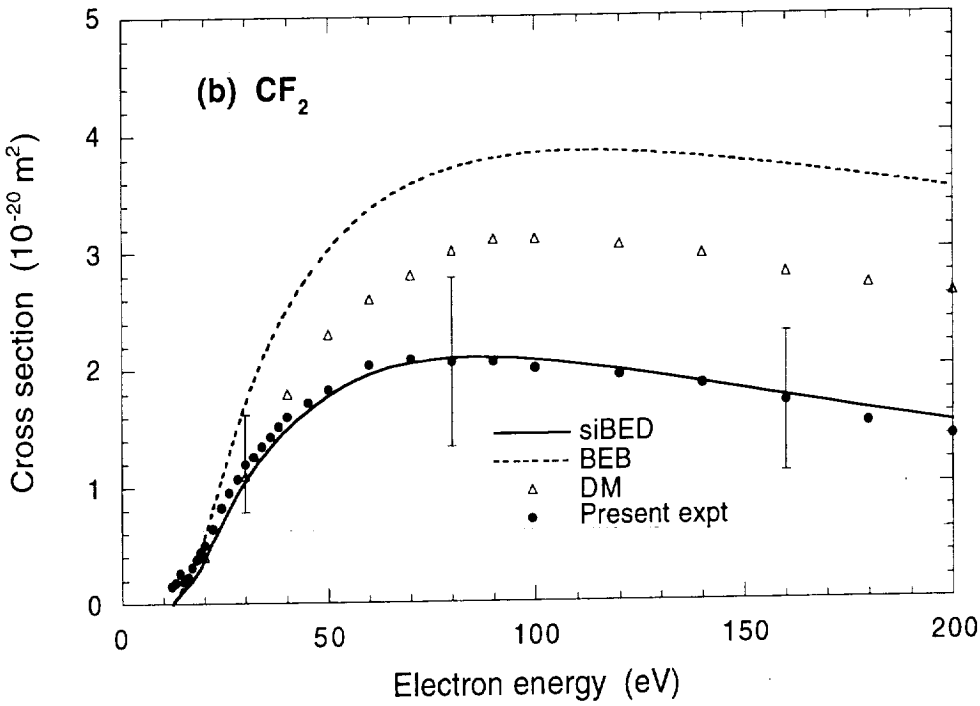

Huo et al. Fig. 1b

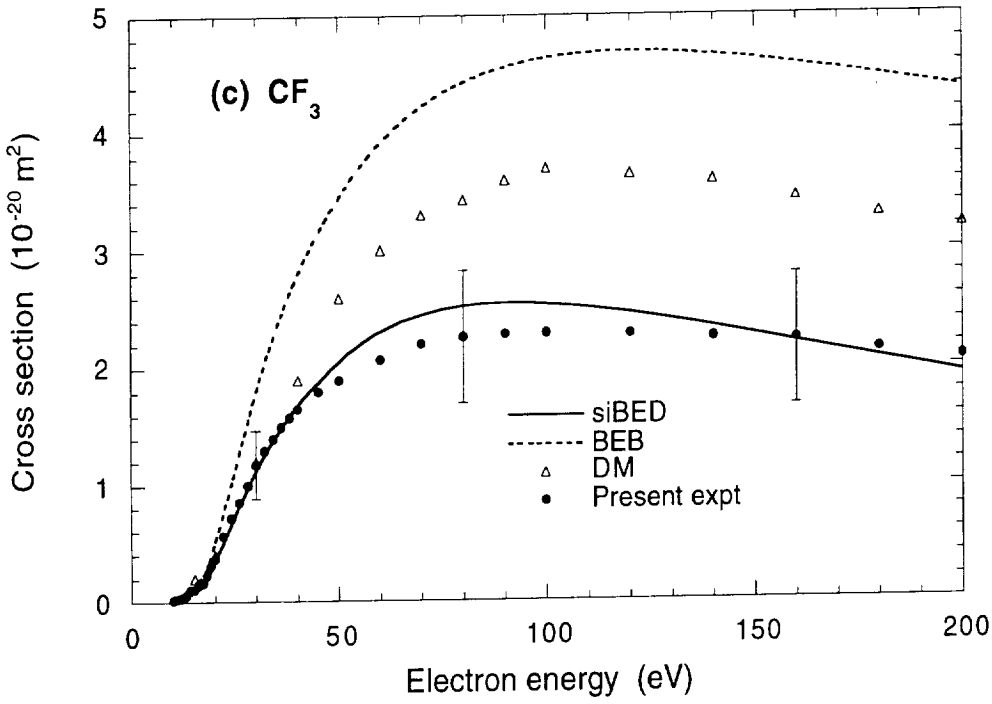

Huo et al. Fig. 1c

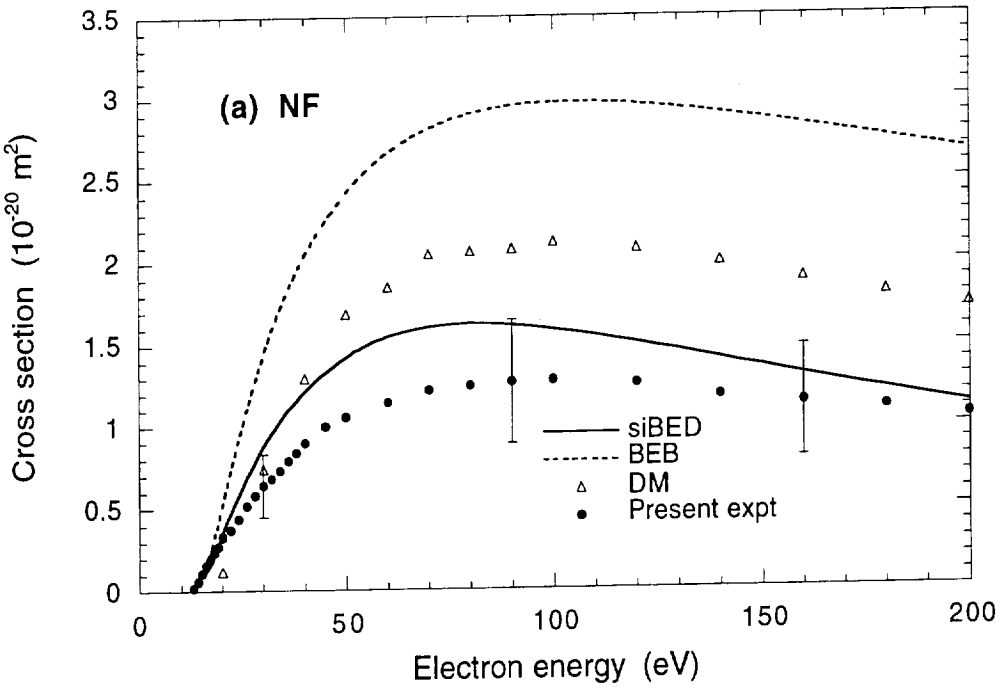

Huo et al. Fig. 2a

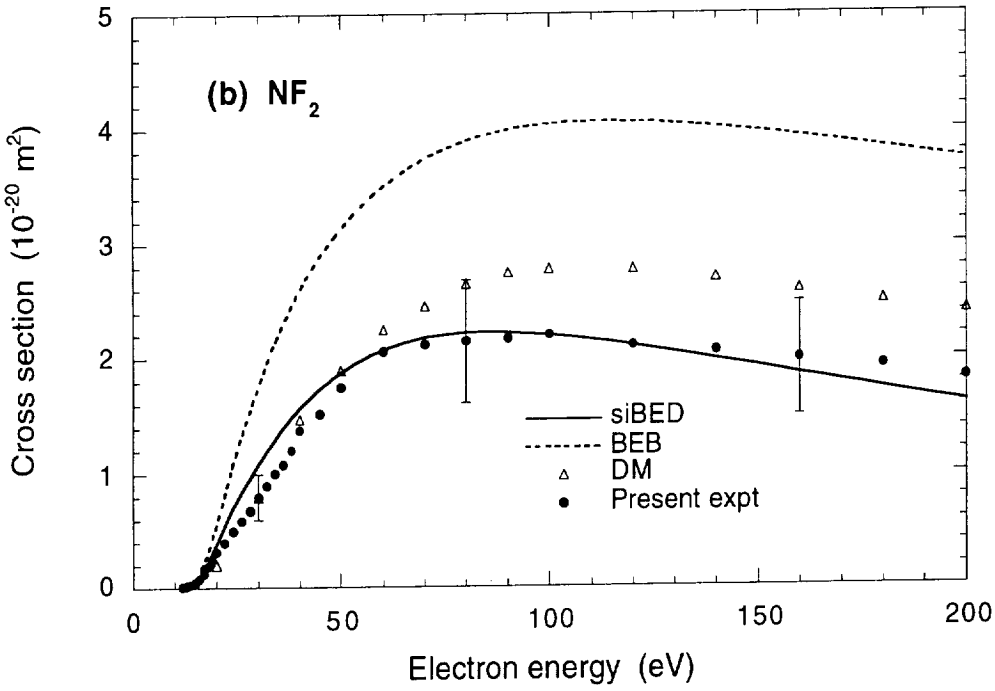

Huo et al. Fig. 2b

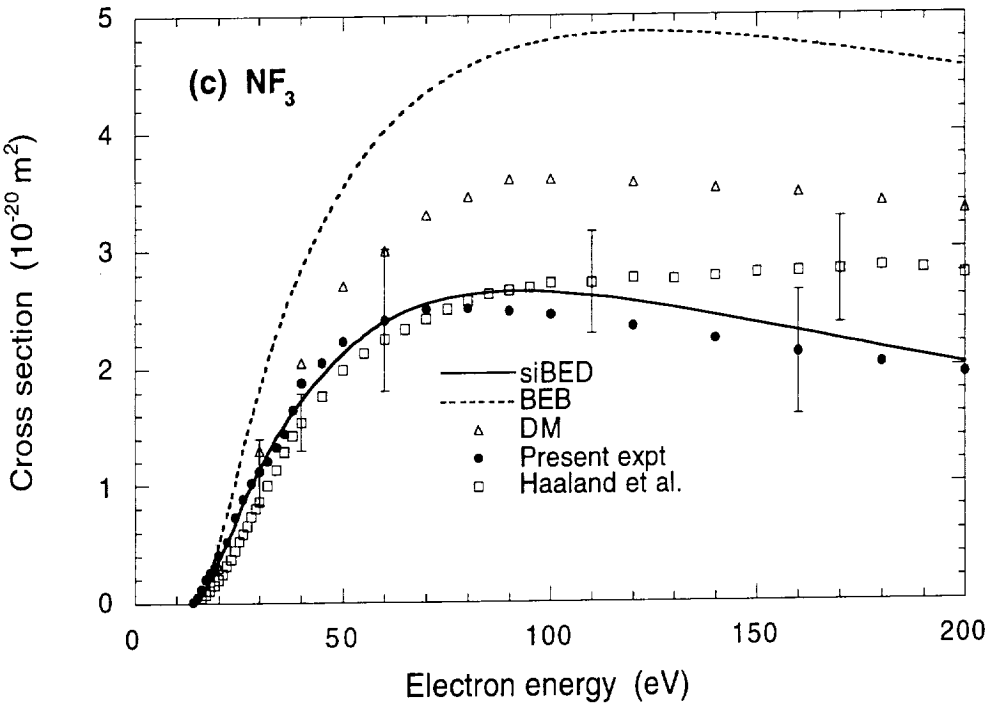

Huo et al. Fig. 2c.